SANDIA REPORT SAND82-0672 • Unlimited Release • UC-60

Printed February 1982

Reprinted July, 1983
Reprinted November 1984

Aeroelastic Stability Analysis of a Darrieus Wind Turbine

David Popelka

Prepared by
Sandia National Laboratories
Albuquerque, New Mexico 87185 and Livermore, California 94550
for the United States Department of Energy
under Contract DE-AC04-76DP00789

Issued by Sandia National Laboratories, operated for the United States Department of Energy by Sandia Corporation.

Printed in the United States of America
Available from
National Technical Information Service
U.S. Department of Commerce
5285 Port Royal Road
Springfield, VA 22161

NTIS price codes
Printed copy: A03
Microfiche copy: A01

SAND82-0672

AEROELASTIC STABILITY ANALYSIS OF A DARRIEUS WIND TURBINE*

David Popelka**
Member Technical Staff
Applied Mechanics Division III
Sandia National Laboratories
Albuquerque, NM 87185

February, 1982

Abstract

An aeroelastic stability analysis has been developed for predicting flutter instabilities on vertical axis wind turbines. This report describes the analytical model and mathematical formulation of the problem as well as the physical mechanism that creates flutter in Darrieus turbines. Theoretical results are compared with measured experimental data from flutter tests of the Sandia 2 Meter turbine. Based on this comparison, the analysis appears to be an adequate design evaluation tool.

---

* This work was performed at Sandia National Laboratories and was supported by the U.S. Department of Energy under contract number DE-AC04-76DP00789.

** Currently Dynamics Specialist at Bell Helicopter Textron, Ft. Worth, Texas.

Table of Contents

Introduction

Tests of a scale model Darrieus wind turbine have shown that under certain conditions, the turbine may experience a flutter instability. Although flutter has not been observed on a full scale turbine, an analysis is required that will guarantee the stability of a future design.

A survey was made of the currently available aeroelastic stability analyses which are listed in Refs. 1-5. The majority of these analyses are complex, exact treatments of the aeroelastic problem. Although these analyses will probably yield accurate results, they are cumbersome to implement and the physical understanding of the flutter problem is easily lost. Ref. 2 is a simplified method which revealed that mass balance of the blade cross section was not important for flutter stability; a finding which has had tremendous impact on blade manufacturing costs.

In this report, an approach was chosen that can give physical insight as well as reasonable numerical results. Test data from the Sandia 2 Meter turbine proved invaluable in guiding the development of the analysis along a path that would yield a maximum of understanding with a minimum amount of mathematical complexity.

Mathematical Formulation of the Flutter Problem

The modal analysis method was used as the basis for the flutter analysis. This approach is used frequently for

analysis of helicopter blade response and was used by Ref. 1 for the vertical axis wind turbine. This method allows the analyst the freedom to describe the structural characteristics of the turbine in minute detail by using NASTRAN finite element modeling techniques to generate the necessary natural frequencies and mode shapes. The general equations of motion for the aeroelastic analysis of the turbine are as follows:

$$[M]\{\ddot{x}\} + [D]\{\dot{x}\} + [K]\{x\} = -\Omega^2[KM]\{x\} - 2\Omega[C]\{\dot{x}\} + [AK]\{x\} + [AD]\{\dot{x}\} + [AM]\{\ddot{x}\} + \{F(t)\} \quad (1)$$

where

$\{X\}$ = structural displacement response

$[M]$ = structural mass matrix

$[D]$ = structural damping matrix (diagonal matrix)

$[K]$ = structural stiffness matrix including centrifugal stiffening

$[KM]$ = centrifugal softening matrix

$[C]$ = Coriolis matrix

$[AK]$ = aerodynamic stiffness matrix

$[AD]$ = aerodynamic damping matrix

$[AM]$ = aerodynamic mass matrix

Ω = turbine rotational speed

$\{F(t)\}$ = time dependent external forces

The forces F(t) consist of harmonic aerodynamic forcing functions which are independent of the structural response. These forces do not affect the stability of the turbine and are therefore neglected.

To utilize modal analysis techniques, the solution to Eq. 1 is taken to be a linear combination of the normal modes of the following equation:

$$[M]\{\ddot{x}\} + [K]\{x\} = 0 \tag{2}$$

This equation represents the structural properties of the turbine and is solved by finite element techniques using the NASTRAN Code. The normal modes contain geometric stiffness effects resulting from centrifugal loading.

If ϕ_i are the mode shapes of Eq. 2, these modes can be assembled into the modal matrix $[\phi]$, and the physical response $\{x\}$ related to the modal response $\{q\}$ as follows:

$$\{x\} = [\phi]\{q\}$$

Substituting this equation into Eq. 1 and then premultiplying by $[\phi]^T$ yields:

$$\begin{aligned}[GI]\{\ddot{q}\} + [2\xi\omega_N GI]\{\dot{q}\} + [GI\omega_N{}^2]\{q\} = {} & -2\Omega[\phi]^T[C][\phi]\{\dot{q}\} - \Omega^2[\phi]^T[KM][\phi]\{q\} \\ & + [\phi]^T[AK][\phi]\{q\} + [\phi]^T[AD][\phi]\{\dot{q}\} \\ & + [\phi]^T[AM][\phi]\{\ddot{q}\}\end{aligned} \tag{3}$$

where:

$\{q\}$ = modal response coordinates

$[GI]$ = diagonal generalized mass matrix

$[2\xi\omega_N GI]$ = diagonal modal damping matrix

$[GI\omega_N{}^2]$ = diagonal generalized stiffness matrix

ξ = structural damping factor

ω_N = natural frequency

Ω = turbine RPM

For very small values of structural damping or for proportional damping, the left hand side of Eq. 3 is completely decoupled as discussed in Ref. 6. Since all terms in Eq. 3 are functions of the modal response coordinates, the right hand side can be combined with the left hand side yielding:

$$[GI-AMB]\{\ddot{q}\} + [2\xi\omega_N GI + CB - ADB]\{\dot{q}\} + [GI\omega_N^2 - AKB + KMB]\{q\} = 0 \quad (4)$$

where:

$$AMB = [\phi]^T[AM][\phi]$$

$$ADB = [\phi]^T[AD][\phi]$$

$$AKB = [\phi]^T[AK][\phi]$$

$$CB = 2\Omega[\phi]^T[C][\phi]$$

$$KMB = \Omega^2[\phi]^T[KM][\phi]$$

Standard eigenvalue routines are used to solve this system of equations for the complex eigenvalues, $\lambda = \sigma + iw$. The real part of the eigenvalue, σ, determines the stability of the mode. A positive value indicates an instability and a negative value indicates a stable configuration. The imaginary component, iw, contains the flutter frequency.

Description of the Flutter Model

A typical NASTRAN model for the flutter analysis is shown in Fig. 1. A single blade is used with a tower that has the proportional torsional stiffness for that blade. The drive train is modeled by a torsional spring which represents the low speed shaft stiffness. The troposkein shaped blade is represented by a series of straight beam elements. To simplify

the calculation of aerodynamic forces, each beam element contains an additional intermediate node as shown in Fig. 1. The distributed aerodynamic loads are computed for the beam element and these forces are lumped to the intermediate node which also contains the concentrated mass properties of the beam element. The cross section of the turbine blade in Fig. 1 shows the relative location of the midchord, elastic axis, and center of mass. The flutter instability involves an interaction between the two modes shown in Fig. 1. These two modes do not include tower translation, so the top and bottom of the tower are pin jointed.

Derivation of the Equations of Motion

The equations of motion for the wind turbine are derived from Newton's laws using the following conditions:

1. All equations are expressed in the rotating coordinate system. This eliminates time-dependent coefficients that are present if the equations are derived in the fixed coordinate system.
2. The turbine blade dynamics are based on concentrated mass particles connected by massless elastic beams.

Fig. 2 illustrates the coordinate systems and degrees of freedom needed to define the blade motion. The "R" coordinate system represents the rotating coordinate system aligned with the undeformed tower and blades. For convenience, at each mass particle on the blade, a local "l" coordinate system is defined

parallel to the "R" system. The "2" coordinate system is aligned with the local curvature of the blade, and is related to the "1" coordinate system by the angle γ as follows:

$$\begin{Bmatrix} i_2 \\ j_2 \\ k_2 \end{Bmatrix} = \begin{bmatrix} \cos\gamma & 0 & -\sin\gamma \\ 0 & 1 & 0 \\ \sin\gamma & 0 & \cos\gamma \end{bmatrix} \begin{Bmatrix} i_1 \\ j_1 \\ k_1 \end{Bmatrix} \tag{5}$$

Coordinate system "3" follows the blade section during elastic deformations. The relation between the "3" coordinate system and the "2" coordinate system is given as:

$$\begin{Bmatrix} i_3 \\ j_3 \\ k_3 \end{Bmatrix} = \begin{bmatrix} 1 & \phi_z & -\phi_y \\ -\phi_z & 1 & \phi_x \\ \phi_y & -\phi_x & 1 \end{bmatrix} \begin{Bmatrix} i_2 \\ j_2 \\ k_2 \end{Bmatrix} \tag{6}$$

The rotations ϕ_x, ϕ_y and ϕ_z are transformed to the "R" coordinate system as shown below:

$$\begin{Bmatrix} \phi_{xr} \\ \phi_{yr} \\ \phi_{zr} \end{Bmatrix} = \begin{bmatrix} \cos\gamma & 0 & \sin\gamma \\ 0 & 1 & 0 \\ -\sin\gamma & 0 & \cos\gamma \end{bmatrix} \begin{Bmatrix} \phi_x \\ \phi_y \\ \phi_z \end{Bmatrix}$$

where ϕ_{xr}, ϕ_{yr}, and ϕ_{zr} are the rotations about the $i_r j_r k_r$ axes.

Referring to Fig. 3, the equations for dynamic equilibrium of a elemental blade section can be written. In the limiting case of an infinitesimal blade section length, a point mass results with the following equations of motion:

$$\bar{F}_1 - \bar{F}_2 = \underline{m\bar{a}} - \bar{F}_{aero} \qquad \text{(Force Equilibrium)} \tag{7}$$

$$\bar{M}_1 - \bar{M}_2 = \underline{\dot{\bar{P}} + \overline{eg_r} \times m\bar{a}} - \bar{M}_{AERO} \qquad \text{(Moment Equilibrium)} \tag{8}$$

The underlined components of the above equation are due to the dynamics of blade motion and are derived below.

For a rotating dynamic system, the position, velocity and acceleration of a particle of mass is given by:

$$\begin{aligned} \bar{r} &= r_p \\ \dot{\bar{r}} &= \dot{r}_p + \omega x r_p \\ \ddot{\bar{r}} &= \ddot{r}_p + \dot{\omega} x r_p + 2\omega x \dot{r}_p + \omega x \omega x r_p \end{aligned} \tag{9}$$

where r_p is the position vector of the concentrated mass and ω is the angular velocity of the rotating coordinate system.

Referring to Figure 2, the position vector of the center of mass of a blade section is:

$$\bar{r} = (r_o + U_x)\, i_r + U_y j_r + U_z k_r + egj_3 \tag{10}$$

The angular velocity of the blade section is

$$\omega_3 = \dot{\phi}_x i_2 + \dot{\phi}_y j_2 + \dot{\phi}_z k_2 + \Omega k_r \tag{11}$$

Transforming the angular velocity to the "3" coordinate system yields,

$$\begin{aligned} \omega_3 = {} & (\dot{\phi}_x - \Omega \sin\gamma - \phi_y \Omega \cos\gamma) i_3 + (\phi_z \Omega \sin\gamma + \dot{\phi}_y + \phi_x \Omega \cos\gamma) j_3 \\ & + (-\Omega \phi_y \sin\gamma + \dot{\phi}_z + \Omega \cos\gamma) k_3 \end{aligned}$$

Beginning with Eq. 9 in coordinate system "3" and using Eqs. 5 and 6 to transform to the "R" coordinate system, the particle velocity expressed in the "R" system is:

$$\begin{aligned} \bar{V} = \dot{\bar{r}} = {} & [\dot{U}_x - \Omega U_y - eg(\Omega + \dot{\phi}_{zr})] i_r \\ & + [\dot{U}_y + \Omega(r_o + U_x) - eg\Omega\phi_{zr}] j_r + [\dot{U}_z + eg\, \dot{\phi}_{xr}] k_r \end{aligned} \tag{12}$$

The acceleration of the particle in the "R" system is given by:

$$\begin{aligned}\bar{a} = \ddot{\bar{r}} = {} & [\ddot{U}_x - 2\Omega\dot{U}_y - (r_o + U_x)\Omega^2 + (\Omega^2\phi_{zr} - \ddot{\phi}_{zr})eg]i_r \\ & + [\ddot{U}_y + 2\Omega\dot{U}_x - \Omega^2 U_y - 2\Omega\dot{\phi}_{zr}eg - \Omega^2 eg]j_r \\ & + [\ddot{U}_z + \ddot{\phi}_{xr}eg]k_r\end{aligned} \tag{13}$$

The inertia force, $m\bar{a}$, is written in matrix form as follows:

$$\begin{aligned}m\bar{a} = {} & \begin{bmatrix} m & 0 & 0 & 0 & 0 & -meg \\ 0 & m & 0 & 0 & 0 & 0 \\ 0 & 0 & m & meg & 0 & 0 \end{bmatrix} \begin{Bmatrix} \ddot{U}_x \\ \ddot{U}_y \\ \ddot{U}_z \\ \ddot{\phi}_{xr} \\ \ddot{\phi}_{yr} \\ \ddot{\phi}_{zr} \end{Bmatrix} + \begin{bmatrix} 0 & -2m\Omega & 0 & 0 & 0 & 0 \\ 2m\Omega & 0 & 0 & 0 & 0 & -2meg\Omega \\ 0 & 0 & 0 & 0 & 0 & 0 \end{bmatrix} \begin{Bmatrix} \dot{U}_x \\ \dot{U}_y \\ \dot{U}_z \\ \dot{\phi}_{xr} \\ \dot{\phi}_{yr} \\ \dot{\phi}_{zr} \end{Bmatrix} \\ & \begin{bmatrix} -m\Omega^2 & 0 & 0 & 0 & m\Omega^2 eg \\ 0 & -m\Omega^2 & 0 & 0 & 0 \\ 0 & 0 & 0 & 0 & 0 \end{bmatrix} \begin{Bmatrix} U_x \\ U_y \\ U_z \\ \phi_{xr} \\ \phi_{yr} \\ \phi_{zr} \end{Bmatrix}\end{aligned} \tag{14}$$

The angular momentum of the blade section is given by:

$$[P_3] = [I_3]\ \{\omega_3\} \tag{15}$$

where $[I_3]$ is the inertia matrix for the blade section and $\{\omega_3\}$ is the angular velocity of the section. The rate of change of angular momentum is given by:

$$\dot{\bar{P}} = [\dot{P}_3] + \{\omega_3\}x[P_3] \tag{16}$$

The inertia matrix for a blade section is expressed in the blade coordinate system as:

$$[I_3] = \begin{bmatrix} I_{xx} & 0 & 0 \\ 0 & I_{yy} & 0 \\ 0 & 0 & I_{zz} \end{bmatrix}$$

The products of inertia are assumed to be small and have been neglected to simplify the equations. Substituting Eq. 11 into Eq. 16 and transforming to the "R" coordinate system results in the following equations in matrix form:

$$\dot{\bar{P}} = \begin{bmatrix} 0 & 0 & 0 & I_{xx}\cos^2\gamma + I_{zz}\sin^2\gamma & 0 & \sin\gamma\cos\gamma(I_{zz} - I_{xx}) \\ 0 & 0 & 0 & 0 & I_{yy} & 0 \\ 0 & 0 & 0 & \sin\gamma\cos\gamma(I_{zz} - I_{xx}) & 0 & I_{xx}\sin^2\gamma + I_{zz}\cos^2\gamma \end{bmatrix} \begin{Bmatrix} \ddot{U}_x \\ \ddot{U}_y \\ \ddot{U}_z \\ \ddot{\phi}_{xr} \\ \ddot{\phi}_{yr} \\ \ddot{\phi}_{zr} \end{Bmatrix}$$

$$+ \begin{bmatrix} 0 & 0 & 0 & 0 & -\Omega[(\sin^2\gamma-\cos^2\gamma)(I_{zz}-I_{xx}) + I_{yy}] & 0 \\ 0 & 0 & 0 & \Omega[(\sin^2\gamma - \cos^2\gamma)(I_{zz} - I_{xx}) + I_{yy}] & 0 & 2\Omega\cos\gamma\sin\gamma(I_{zz}-I_{xx}) \\ 0 & 0 & 0 & 0 & -2\Omega\cos\gamma\sin\gamma(I_{zz}-I_{xx}) & 0 \end{bmatrix} \begin{Bmatrix} \dot{U}_x \\ \dot{U}_y \\ \dot{U}_z \\ \dot{\phi}_{xr} \\ \dot{\phi}_{yr} \\ \dot{\phi}_{zr} \end{Bmatrix}$$

$$+ \begin{bmatrix} 0 & 0 & 0 & \Omega^2[I_{xx}\sin^2\gamma + I_{zz}\cos^2\gamma - I_{yy}] & 0 & 0 \\ 0 & 0 & 0 & 0 & \Omega^2[(\cos^2\gamma - \sin^2\gamma)(I_{zz} - I_{xx})] & 0 \\ 0 & 0 & 0 & 0 & 0 & 0 \end{bmatrix} \begin{Bmatrix} U_x \\ U_y \\ U_z \\ \phi_{xr} \\ \phi_{yr} \\ \phi_{zr} \end{Bmatrix} \quad (17)$$

The center of mass offset from the elastic axis creates a moment about the elastic axis. The mass offset expressed in the "R" coordinate system is:

$$\bar{eg}_r = eg[(-\phi_z \cos\gamma + \phi_x \sin\gamma)i_r + j_r + (\phi_z \sin\gamma + \phi_x \cos\gamma)k_r] \tag{18}$$

The moment due to the mass offset is:

$$\bar{eg}_r \times m\bar{a} = \begin{bmatrix} i_r & j_r & k_r \\ eg(-\phi_z \cos\gamma + \phi_x \sin\gamma) & eg & eg(\phi_z \sin\gamma + \phi_x \cos\gamma) \\ m\bar{a}_x & m\bar{a}_y & m\bar{a}_z \end{bmatrix} \tag{19}$$

Substituting Eq. 14 into Eq. 19 yields:

$$\bar{eg}_r \times m\bar{a} = \begin{bmatrix} 0 & 0 & meg & meg^2 & 0 & 0 \\ 0 & 0 & 0 & 0 & 0 & 0 \\ -meg & 0 & 0 & 0 & 0 & meg^2 \end{bmatrix} \begin{Bmatrix} \ddot{U}_x \\ \ddot{U}_y \\ \ddot{U}_z \\ \ddot{\phi}_{xr} \\ \ddot{\phi}_{yr} \\ \ddot{\phi}_{zr} \end{Bmatrix} + \tag{20}$$

$$\begin{bmatrix} 0 & 0 & 0 & 0 & 0 & 0 \\ 0 & 0 & 0 & 0 & 0 & 0 \\ 0 & 2meg\Omega & 0 & 0 & 0 & 0 \end{bmatrix} \begin{Bmatrix} \dot{U}_x \\ \dot{U}_y \\ \dot{U}_z \\ \dot{\phi}_{xr} \\ \dot{\phi}_{yr} \\ \dot{\phi}_{zr} \end{Bmatrix} + \begin{bmatrix} 0 & 0 & 0 & m\Omega^2 eg^2 & -mr_o\Omega^2 eg & 0 \\ 0 & 0 & 0 & -mr_o\Omega^2 eg & 0 & 0 \\ m\Omega^2 eg & 0 & 0 & 0 & 0 & 0 \end{bmatrix} \begin{Bmatrix} U_x \\ U_y \\ U_z \\ \phi_{xr} \\ \phi_{yr} \\ \phi_{zr} \end{Bmatrix}$$

The complete equations of motion are assembled from equations 14, 17, and 20 and are written as follows:

$$
\begin{Bmatrix} F_{XR} \\ F_{YR} \\ F_{ZR} \\ M_{XR} \\ M_{YR} \\ M_{ZR} \end{Bmatrix} =
\begin{bmatrix}
m & 0 & 0 & 0 & 0 & -meg \\
0 & m & 0 & 0 & 0 & 0 \\
0 & 0 & m & meg & 0 & 0 \\
0 & 0 & meg & meg^2 + I_{xx}\cos^2\gamma + I_{zz}\sin^2\gamma & 0 & \sin\gamma\cos\gamma(I_{zz} - I_{xx}) \\
0 & 0 & 0 & 0 & I_{yy} & 0 \\
-meg & 0 & 0 & \sin\gamma\cos\gamma(I_{zz} - I_{xx}) & 0 & meg^2 + I_{xx}\sin^2\gamma + I_{zz}\cos^2\gamma
\end{bmatrix}
\begin{Bmatrix} \ddot{U}_x \\ \ddot{U}_y \\ \ddot{U}_z \\ \ddot{\phi}_{xr} \\ \ddot{\phi}_{yr} \\ \ddot{\phi}_{zr} \end{Bmatrix}
$$

$$
-
\begin{bmatrix}
0 & -2m\Omega & 0 & 0 & 0 & 0 \\
2m\Omega & 0 & 0 & 0 & 0 & -2m\Omega eg \\
0 & 0 & 0 & 0 & 0 & 0 \\
0 & 0 & 0 & 0 & \Omega[\sin^2\gamma - \cos^2\gamma)(I_{xx} - I_{zz}) - I_{yy}] & 0 \\
0 & 0 & 0 & -\Omega[(\sin^2\gamma - \cos^2\gamma)(I_{xx} - I_{zz}) - I_{yy}] & 0 & -2\Omega\cos\gamma\sin\gamma(I_{xx} - I_{zz}) \\
0 & 2meg\Omega & 0 & 0 & 2\Omega\sin\gamma\cos\gamma(I_{xx} - I_{zz}) & 0
\end{bmatrix}
\begin{Bmatrix} \dot{U}_x \\ \dot{U}_y \\ \dot{U}_z \\ \dot{\phi}_{xr} \\ \dot{\phi}_{yr} \\ \dot{\phi}_{zr} \end{Bmatrix}
$$

$$
-
\begin{bmatrix}
-m\Omega^2 & 0 & 0 & 0 & 0 & m\Omega^2 eg \\
0 & -m\Omega^2 & 0 & 0 & 0 & 0 \\
0 & 0 & 0 & 0 & 0 & 0 \\
0 & 0 & 0 & meg^2\Omega^2 + \Omega^2[I_{xx}\sin^2\gamma + I_{zz}\cos^2\gamma - I_{yy}] & -mr_o\Omega^2 eg & 0 \\
0 & 0 & 0 & -mr_o\Omega^2 eg & \Omega^2[(\cos^2\gamma - \sin^2\gamma)(I_{zz} - I_{xx})] & 0 \\
m\Omega^2 eg & 0 & 0 & 0 & 0 & 0
\end{bmatrix}
\begin{Bmatrix} U_x \\ U_y \\ U_z \\ \phi_{xr} \\ \phi_{yr} \\ \phi_{zr} \end{Bmatrix} \quad (21
$$

The first portion of Eq. 21 is the mass matrix for the blade section, which is represented by [M] in Eq. 1. The second matrix in Eq. 21 is the Coriolis matrix, which appears as [C] in Eq. 1. The last portion of Eq. 21 is the centrifugal softening matrix, or [KM] in Eq. 1.

For most turbine analyses, the blade inertias I_{XX}, I_{YY}, I_{ZZ} are not included in the NASTRAN model and are therefore not used in the flutter analysis. However, they are included in this derivation for completeness.

Derivation of Aerodynamic Loads

The aerodynamic loads acting on the turbine blades are derived using unsteady aerodynamic theory as discussed in Refs. 7-10. These references cite Theodorsen's original work on a two-dimensional airfoil oscillating in a steady air stream. This theory accounts for all possible motions of the blade section that will produce aerodynamic loads.

Several simplifying assumptions, listed below, are made for the airload calculations:

1) Two-dimensional strip theory assumed applicable
2) No stall considered
3) Chord line and zero-lift line assumed to coincide
4) No inflow permitted through the turbine
5) Blade relative wind velocity assumed constant during turbine rotation
6) Aerodynamic center located at quarter chord point

7) Turbine wake not modeled

8) Small angles assumed, linearized aerodynamic equations

As outlined in Ref. 10, the unsteady lift, moment, and drag acting on a blade section are given by the following equations:

$$L = \frac{ao}{2}\rho b V^2 \left\{ CK\left[\frac{-2\dot{h}}{V} + (1 - 2a)\frac{b}{V}\dot{\theta} + 2\theta\right] - \frac{b}{V^2}\ddot{h} - \frac{b^2 a\ddot{\theta}}{V^2} + \frac{b}{V}\dot{\theta}\right\} \quad (22)$$

$$M = \frac{-ao}{2}\rho b^2 V^2 \left\{ \frac{ab\ddot{h}}{V^2} + (1 + 2a)\frac{1}{V}CK\dot{h} + (1/8 + a^2)\frac{b^2}{V^2}\ddot{\theta} - [a - \tfrac{1}{2} + 2(\tfrac{1}{4} - a^2)CK]\frac{b}{V}\dot{\theta} - (1 + 2a)CK\theta\right\} \quad (23)$$

$$D = \tfrac{1}{2}\rho V^2 c\, Cdo \quad (24)$$

where:

- a = nondimensional distance from elastic axis to midchord (positive if elastic axis is aft of midchord, expressed as a fraction of b)
- ao = lift curve slope
- b = 1/2 chord length
- c = chord length
- Cdo = drag coefficient for airfoil
- CK = Theodorsen's lift deficiency function
- D = drag of airfoil (per unit span)
- h = vertical translation of the airfoil at elastic axis (positive up)
- L = unsteady lift at elastic axis (per unit span)
- M = unsteady moment at elastic axis (per unit span)
- V = relative wind velocity for blade section, $\approx Vo + \Omega r_o$
- Vo = wind velocity
- θ = pitch rotation of the airfoil (positive nose-up)
- ρ = air density

The expressions for $\dot{h}$ and $\ddot{h}$ are obtained from Eqs. 12 and 13 and are then resolved into the "2" coordinate system to give:

$$\begin{aligned}\dot{h} &= (\dot{U}_x \sin\gamma - \Omega U_y \sin\gamma + \dot{U}_z \cos\gamma)\, k_2 \\ \ddot{h} &= (\ddot{U}_x \sin\gamma - 2\Omega \dot{U}_y \sin\gamma - (r_o + U_x)\, \Omega^2 \sin\gamma + \ddot{U}_z \cos\gamma)\, k_2\end{aligned} \tag{25}$$

The geometric pitch of the airfoil is given by the following equations:

$$\begin{aligned}\theta &= (\phi_{xr} \cos\gamma - \phi_{zr} \sin\gamma) i_2 \\ \dot{\theta} &= (\dot{\phi}_{xr} \cos\gamma - \dot{\phi}_{zr} \sin\gamma) i_2 \\ \ddot{\theta} &= (\ddot{\phi}_{xr} \cos\gamma - \ddot{\phi}_{zr} \sin\gamma) i_2\end{aligned} \tag{26}$$

Eqs. 25 and 26 are substituted into Eqs. 22 and 23 to give the lift and moment acting on the blade section. In Eq. 22, the lift can be separated into two components. The first component is the circulatory lift, L_c, which depends on the value of CK. This component of the lift vector acts perpendicular to the relative wind and is the result of circulation produced by the lifting airfoil. The second component is the noncirculatory lift, L_{NC}, which includes the "apparent mass" of the air stream and acts perpendicular to the chord line of the airfoil.

Figure 4 shows the aerodynamic loads acting on a typical blade cross section. The lift, drag, and moment can be resolved into the blade coordinate system which yields:

$$F_z = (L_c + D\alpha + L_{NC})k_3$$

$$F_y = (L_c\alpha - D)j_3 \qquad (27)$$

$$M_x = Mi_3$$

The angle of attack, α, is composed of the geometric pitch angle, θ, plus the induced angle of attack, β. The induced angle of attack is the angle due to blade motion, and is the ratio of the blade vertical velocity to the horizontal velocity. The equation for α, is as follows:

$$\alpha = \phi_{xr}\cos\gamma - \phi_{zr}\sin\gamma - [(\dot{U}_x\sin\gamma - \Omega U_y\sin\gamma + \dot{U}_z\cos\gamma)]/V \qquad (28)$$

Substituting Eqs. 22, 23, 24, and 28 into Eq. 27 yields the aerodynamic forces in the blade coordinate system. These forces are then resolved into the "R" coordinate system by using Eqs. 5 and 6.

The final expression for the aerodynamic loads are written in matrix form as follows:

$$
\begin{Bmatrix} F_{xr} \\ F_{yr} \\ F_{zr} \\ M_{xr} \\ M_{yr} \\ M_{zr} \end{Bmatrix} =
\begin{bmatrix}
-A_1 bS\gamma^2 & 0 & -A_1 bS\gamma C\gamma & -A_1 b^2 aC\gamma S\gamma & 0 & A_1 b^2 aS\gamma^2 \\
0 & 0 & 0 & 0 & 0 & 0 \\
-A_1 bS\gamma C\gamma & 0 & -A_1 bC\gamma^2 & -A_1 b^2 aC\gamma^2 & 0 & A_1 b^2 aS\gamma C\gamma \\
-A_1 b^2 aS\gamma C\gamma & 0 & -Ab^2 aC\gamma^2 & -A_6 bC\gamma^2 & 0 & A_6 bS\gamma C\gamma \\
0 & 0 & 0 & 0 & 0 & 0 \\
A_1 b^2 aS\gamma^2 & 0 & A_1 b^2 aS\gamma C\gamma & A_6 bS\gamma C\gamma & 0 & -A_6 bS\gamma^2
\end{bmatrix}
\begin{Bmatrix} \ddot{U}_x \\ \ddot{U}_y \\ \ddot{U}_z \\ \ddot{\phi}_{xr} \\ \ddot{\phi}_{yr} \\ \ddot{\phi}_{zr} \end{Bmatrix}
$$

$$
\begin{bmatrix}
-A_1 C_K 2VS\gamma^2 + A_3 S\gamma^2 & A_1 2b\Omega S\gamma^2 & -A_1 2VCKC\gamma S\gamma + A_3 C\gamma S\gamma & A_1 bVC\gamma S\gamma + A_7 S\gamma C\gamma & 0 & -A_1 bVS\gamma^2 - A_7 S\gamma^2 \\
0 & 0 & 0 & 0 & 0 & 0 \\
-A_1 CK2VS\gamma C\gamma + A_3 S\gamma C\gamma & -A_1 2b\Omega S\gamma C\gamma & -A_1 2VCKC\gamma^2 + A_3 C\gamma^2 & A_1 bVC\gamma^2 + A_7 C\gamma^2 & 0 & -A_1 bVS\gamma C\gamma - A_7 S\gamma C\gamma \\
-A_1 b(1 + 2a)CKVS\gamma C\gamma & A_1 b^2 a2\Omega S\gamma C\gamma & -A_1 b(1 + 2a)CKVC\gamma^2 & A_5 b^2 VC\gamma^2 & 0 & -A_5 b^2 VS\gamma C\gamma \\
0 & 0 & 0 & 0 & 0 & 0 \\
A_1 b(1 + 2a)CKVS\gamma^2 & -A_1 b^2 a2\Omega S\gamma^2 & A_1 b(1 + 2a)CKVC\gamma S\gamma & -A_5 b^2 VS\gamma C\gamma & 0 & A_5 b^2 VS\gamma^2
\end{bmatrix}
\begin{Bmatrix} \dot{U}_x \\ \dot{U}_y \\ \dot{U}_z \\ \dot{\phi}_{xr} \\ \dot{\phi}_{yr} \\ \dot{\phi}_{zr} \end{Bmatrix}
$$

$$
\begin{bmatrix}
A_1 b\Omega^2 S\gamma^2 & A_1 CK2V\Omega S\gamma^2 - A_3 \Omega S\gamma^2 & 0 & A_1 CK2V^2 S\gamma C\gamma - A_3 VS\gamma C\gamma & A_1 br_o \Omega^2 S\gamma C\gamma & -A_3 V - A_1 2CKV^2 S\gamma^2 + A_3 VS\gamma^2 \\
0 & 0 & 0 & -A_1 br_o \Omega^2 S\gamma C\gamma & 0 & A_1 br_o \Omega^2 S\gamma^2 \\
A_1 b\Omega^2 S\gamma C\gamma & A_1 CK2V\Omega S\gamma C\gamma - A_3 \Omega S\gamma C\gamma & 0 & A_1 CK2V^2 C\gamma^2 - A_3 VC\gamma^2 + A_3 V & -A_1 br_o \Omega^2 S\gamma^2 & -A_1 CK2V^2 S\gamma C\gamma + A_3 VS\gamma C\gamma \\
A_1 b^2 a\Omega^2 S\gamma C\gamma & A_4 \Omega S\gamma C\gamma & 0 & A_4 VC\gamma^2 & 0 & -A_4 VC\gamma S\gamma \\
0 & 0 & 0 & A_1 b^2 ar_o \Omega^2 S\gamma^2 & 0 & 0 \\
-A_1 b^2 a\Omega^2 S\gamma^2 & -A_4 \Omega S\gamma^2 & 0 & -A_4 VC\gamma S\gamma & 0 & A_4 VS\gamma^2
\end{bmatrix}
$$

where:

$$A_1 = \rho b a_0 \Delta L/2.$$

$$A_3 = 1/2\ \rho V^2 b C d o \Delta L$$

$$A_4 = A_1(1 + 2a)\ VCKb$$

$$A_5 = A_1[a - 1/2 + 2(1/4 - a^2)CK]$$

$$A_6 = A_1(1/8 + a^2)b^2$$

$$A_7 = A_1 CK(1 - 2a)bV$$

$$S\gamma = \sin\gamma$$

$$C\gamma = \cos\gamma$$

The first matrix in Eq. 29 is the aerodynamic mass matrix corresponding to [AM] in Eq. 1. The second matrix is the aerodynamic damping matrix which is represented by [AD] in Eq. 1. The last portion is the aerodynamic stiffness matrix denoted by [AK]. Note that neither [AD] nor [AK] are symmetric because the aerodynamic forces do not constitute a conservative system.

The aerodynamic loads in Eq. 29 include the Theodorsen Function, CK, which is a measure of the unsteadiness of the flow field. The parameter, CK, is a complex number which alters the phase angle between the airfoil oscillation and the resultant aerodynamic forces. Its value is dependent on the reduced frequency, or Strouhal number. For the flutter instabilities observed on the VAWT, the Strouhal number is very low which renders CK equal to unity. This corresponds to a "quasi-steady" flow field which appears to be an adequate representation of the aerodynamic loads for the VAWT flutter problem.

Flutter Test Program

To verify the accuracy of the flutter analysis, a flutter test program was conducted. This test program utilized the Sandia 2 Meter turbine with several sets of aluminum blades.

These test were conducted in the following manner:

1. The non-rotating blade frequencies were measured for comparison with the NASTRAN model of the turbine. The modal damping of the turbine was also measured but it was difficult to get a repeatable value. Generally, the modal damping varied from .1% to .4% critical. A value of .35% was used in the analysis.
2. The turbine speed was set and an impulse was applied to the turbine through the brake system to trigger the flutter instability. A torque meter was used to record the resulting torque oscillation which increased during a flutter instability and decayed to a stable configuration.

The mechanism that creates flutter is clearly shown in slow motion films of the flutter instability. The instability is due to coupling between the flatwise bending and torsion mode shown in Fig. 1. The flatwise bending mode involves radial motion of the blade which creates Coriolis forces that amplify the response of the torsion mode. The resulting elastic deflections cause changes in the aerodynamic forces which add energy to the vibrating blade and create flutter.

Correlation of Theory and Experiment

The flutter analysis was verified by comparing the theoretical results with measured test data. Fig. 5 shows the flutter stability for the two meter turbine with three aluminum blades (NACA 0012, CHORD = 2.91 in) and a truss tower. This figure shows the variation in modal damping and modal frequency with turbine speed. The modal damping curve was calculated with zero structural damping. This damping curve is very shallow which means that small changes in the structural damping have a large influence on the flutter speed. The theoretical flutter speed was found by adding .35% structural damping to the modal damping curve, giving 850 RPM as the flutter speed. This is in fair agreement with the measured flutter speed of 745 RPM. The calculated flutter frequency, 18.5 Hz, agrees well with the measured flutter frequency, 18 Hz.

The turbine was modified by replacing the truss tower with a torsionally stiff pipe tower. The flutter instability did not occur in tests up to 900 RPM. Theoretical results agree with this data.

Wind speed effects were evaluated by testing the turbine in 25 mph winds. The turbine configuration consisted of three aluminum blades (NACA 0012, CHORD = 2.91 in) and a truss tower. Fig. 6 shows the measured flutter speed to be in the range of 705-720 RPM at a flutter frequency of 18 Hz. The theoretical results indicate flutter at 695 RPM at a frequency of 16.5 Hz. The theory predicts that the wind velocity has a

larger influence on the flutter speed than the test results indicate. This is probably due to the simplifying assumptions in the aerodynamic load calculations.

A larger set of blades (NACA 0012, CHORD = 3.47 in) was installed on the two meter turbine with the truss tower as shown in Fig. 7. This set of blades did not flutter up to speeds of 1050 RPM. The analysis, however, predicts flutter at 1000 RPM. This disagrees with the test results, but since flutter was not observed in the test, the magnitude of the theoretical error is unknown.

Fig. 8 displays the flutter results for the small blades (NACA 0015, CHORD = 2.31 in). Flutter was noted at 777 RPM at a frequency of 18.5 Hz. Theoretically the flutter speed is 865 RPM at a frequency of 18.7 Hz, which correlates well with the test data.

The stability of the 17 Meter Sandia turbine is shown in Fig. 9. The calculated flutter speed is 176 RPM at 4.5 Hz, which is well above the 50 RPM operating speed.

These results indicate that the analysis is capable of assessing the effect of turbine design changes on flutter speed. The stability trends are predicted accurately by the program and the numerical results are sufficiently accurate to establish confidence in the analysis.

Conclusions

The analysis developed here has shown to be a useful tool for understanding and predicting flutter of Darrieus, vertical axis wind turbines. Additional test data is needed to fully verify the accuracy of the analysis and to establish error bounds. The analysis is potentially weak in the areas of aerodynamic force calculation since several simplifying assumptions have been made. A more complex aerodynamic model would improve the predictive capability of the model.

Several observations have been made based on the results of the analysis and tests:

1. Flutter is a result of aeroelastic coupling of two primary blade modes; the first flatwise bending mode and the first torsion mode.
2. Flutter does not require that two blade modes be in resonance. The frequencies of the flatwise mode and the torsion mode do not converge in the operating RPM range. However, increasing the separation of the flatwise mode and the torsion mode increases the flutter RPM.
3. Tower and drive train torsional stiffness affect the torsion mode frequency which affects the flutter RPM.
4. Flutter occurs at a frequency very near the flatwise mode frequency.
5. Wind velocity reduces the flutter RPM, but for operational wind speeds, the effect is relatively small.

Recommendations for Future Work

The flutter problem should be investigated further with a comprehensive program of testing and theoretical investigations. It is recommended that the following problem areas be addressed:

1. Determine the effect of chordwise mass balance on the flutter stability. This will involve the fabrication of blades with significant chordwise center of gravity offset. Ref. 2 predicts that mass offset has little influence on flutter stability. This should be verified with test data and results from the analysis.
2. Study the effect of blade frequency placement and the role of tower torsional stiffness on flutter stability.
3. Evaluate the effect of wind velocity on flutter stability in greater detail. Very high, short duration wind gusts may reduce the flutter RPM.
4. Modify the aerodynamic load model to account for stall, dynamic inflow, turbine wake effects, and periodic variation in relative wind velocity.

Acknowledgement

The author would like to acknowledge the technical support on this project from R. C. Reuter, D. W. Lobitz, W. N. Sullivan, J. R. Koteras, and T. M. Leonard. Assistance during the test program was provided by M. H. Worstell, J. D. Burkhardt, and L. H. Wilhelmi.

References

1. A. J. Vollan, "The Aeroelastic Behavior of Large Darrius-Type Wind Energy Converters Derived from the Behavior of a 5.5 Meter Rotor," Dornier System GMBH, German Federal Republic

2. Norman D. Ham, "Aeroelastic Analysis of the Troposkien-Type Wind Turine," Sandia Laboratories, SAND 77-0026, April, 1977.

3. Krishna Rao Kaza, Raymond G. Kvaternik, "Aeroelastic Equations of Motion of a Darrius Vertical Axis Wind Turbine Blade," NASA TM-79295, December, 1979.

4. J. Wendell, "Aeroelastic Stability of Wind Turbine Rotor Blades," MIT Aeroelastic and Structures Research Laboratory, Department of Aeronautics and Astronautics, Cambridge, Massachusetts, September, 1978.

5. William Warmbrodt and Peritz Friedman, "Coupled Rotor/Tower Aeroelastic Analysis of Large Horizontal Axis Wind Turbine," AIAA Journal, Vol 18, No. 9, September, 1980.

6. Leonard Meirovitch, Analytical Methods in Vibrations, The Macmillan Co., Collier-Macmillan Limited, London, 1969.

7. Raymond L. Blisplinghoff, Holt Ashley, Robert L. Halfman, Aeroelasticity, Addison-Wesley Publishing Company, Inc., Reading Massachusetts, 1955.

8. Norman Abramson, An Introduction to the Dynamics of Airplanes, Dover Publications, Inc., New York, 1958.

9. Y. C. Fung, An Introduction to the Theory of Aeroelasticity, Dover Publications Inc., New York, 1969.

10. Robert Scanlan and Robert Rosenbaum, Aircraft Vibration and Flutter, Dover Publications, New York.

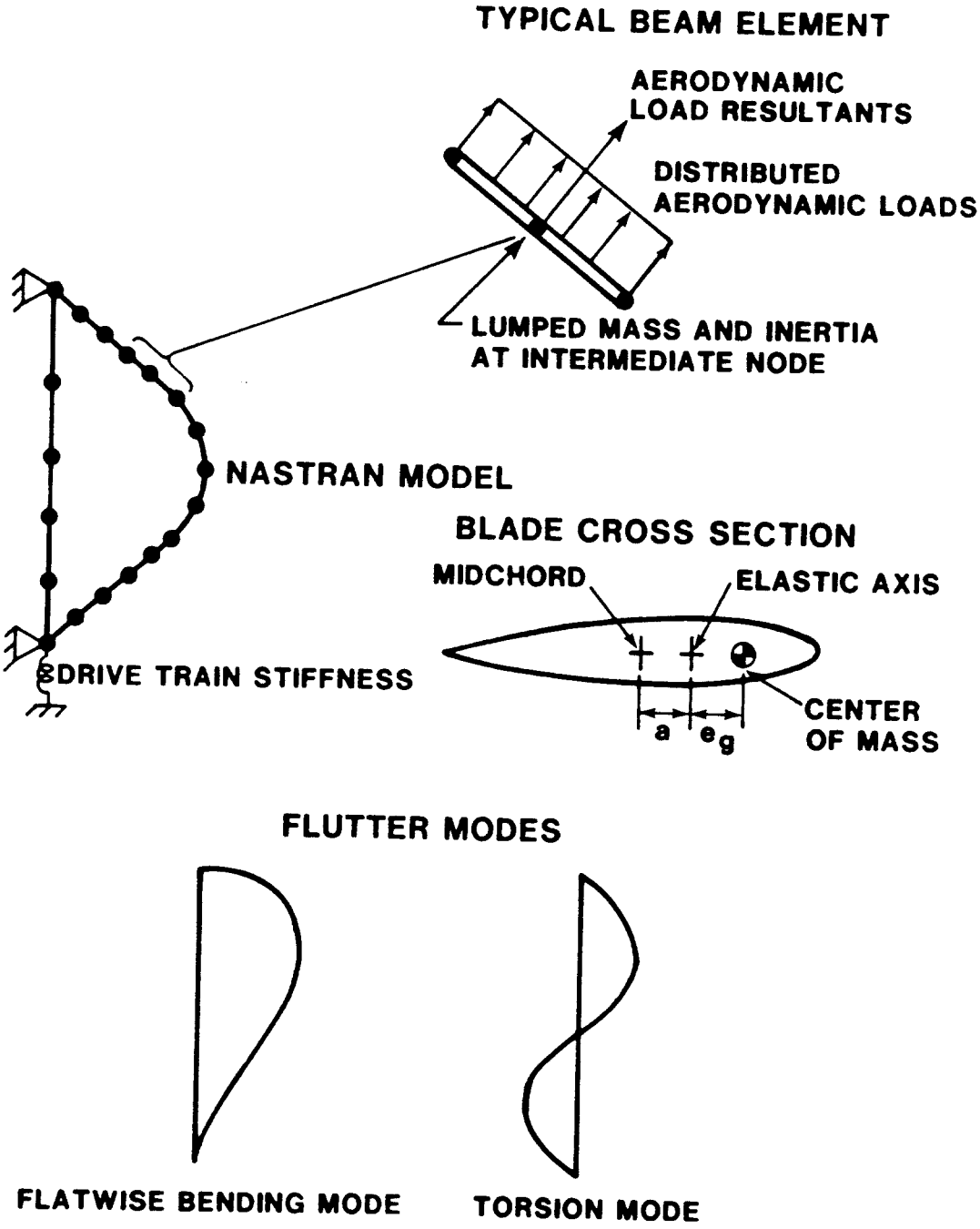

Figure 1. Mathematical Modeling Technique for the Flutter Analysis

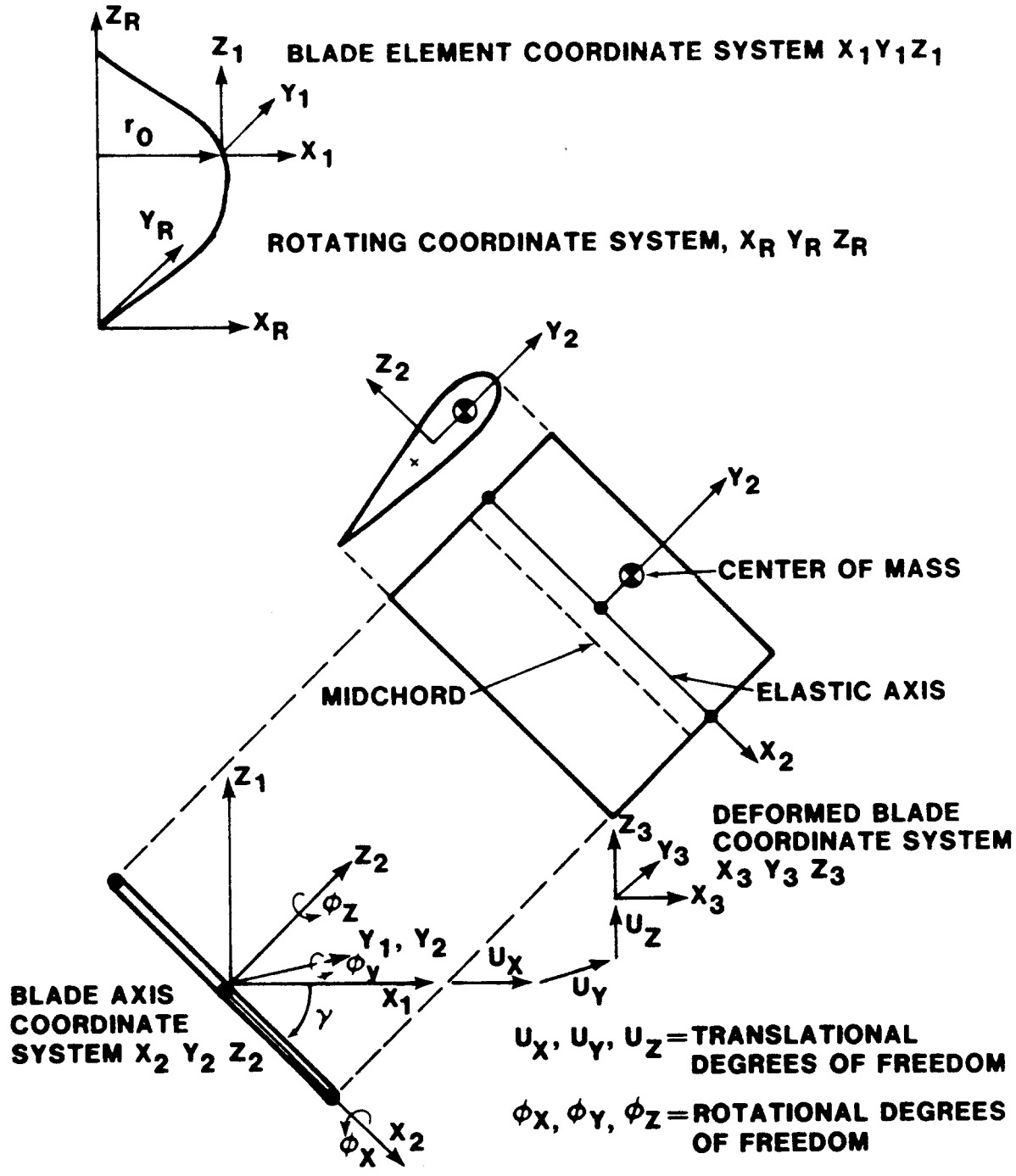

Figure 2. Coordinate Systems and Degrees of Freedom used in the Flutter Analysis

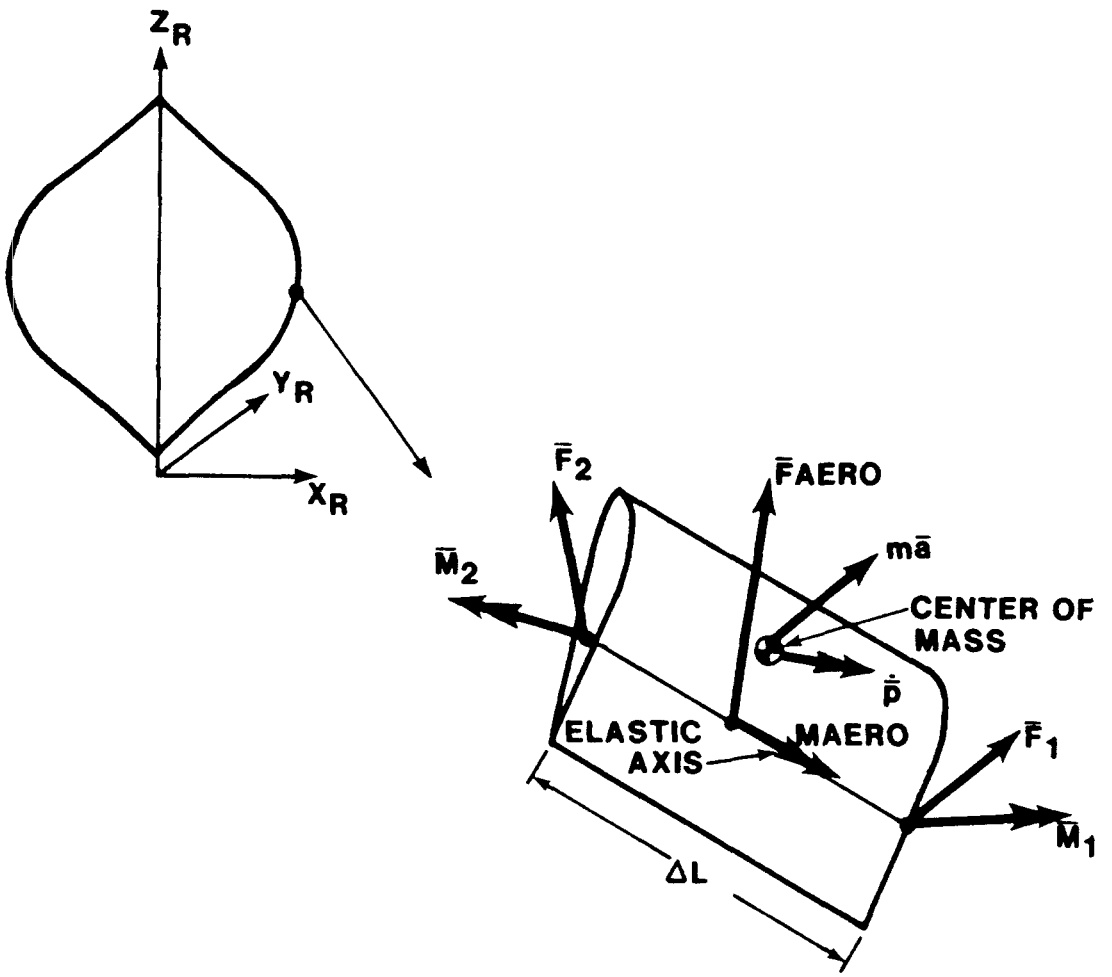

$\bar{M}AERO$ = AERODYNAMIC MOMENT ABOUT ELASTIC AXIS

$\bar{F}AERO$ = AERODYNAMIC FORCE AT ELASTIC AXIS

$m\bar{a}$ = INERTIA FORCE AT CENTER OF MASS

$\dot{\bar{p}}$ = RATE OF CHANGE OF ANGULAR MOMENTUM VECTOR

$\bar{M}1$, $\bar{M}2$ = MOMENT RESULTANTS AT INBOARD AND OUTBOARD ENDS OF SEGMENT

$\bar{F}1$, $\bar{F}2$ = FORCE RESULTANTS AT INBOARD AND OUTBOARD ENDS OF SEGMENT

Figure 3. Force and Moment Equilibrium for a Blade Element

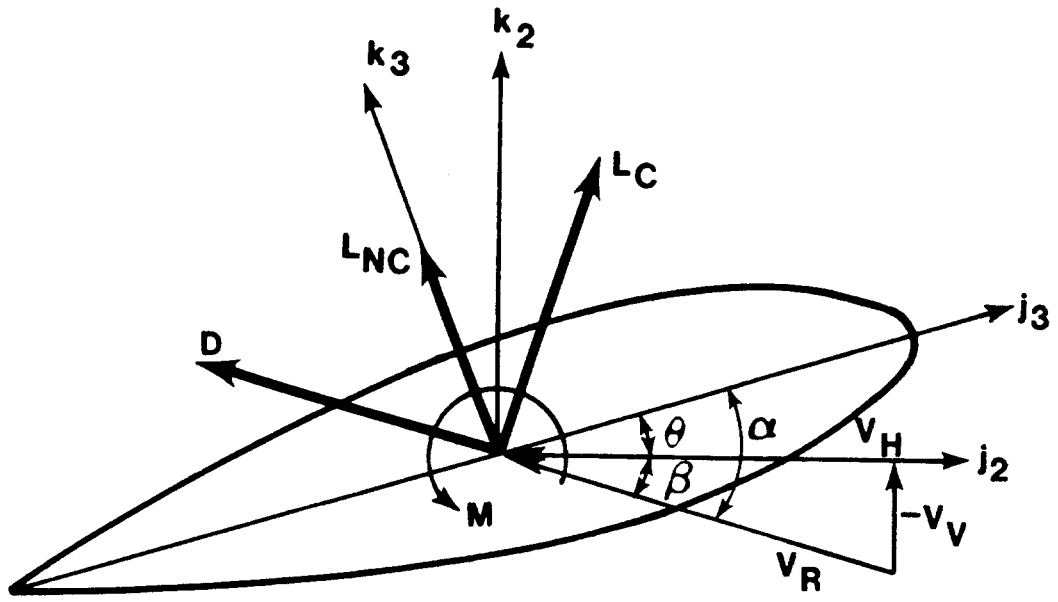

L_C = CIRCULATORY LIFT
L_{NC} = NON-CIRCULATORY LIFT
D = AERODYNAMIC DRAG
M = AERODYNAMIC MOMENT
V_V = VERTICAL VELOCITY
V_H = HORIZONTAL VELOCITY
α = ANGLE OF ATTACK = $\beta + \theta$
θ = GEOMETRIC PITCH
β = INDUCED ANGLE OF ATTACK
V_R = RELATIVE WIND VELOCITY

Figure 4. Aerodynamic Forces and Moments Acting on an Airfoil Section

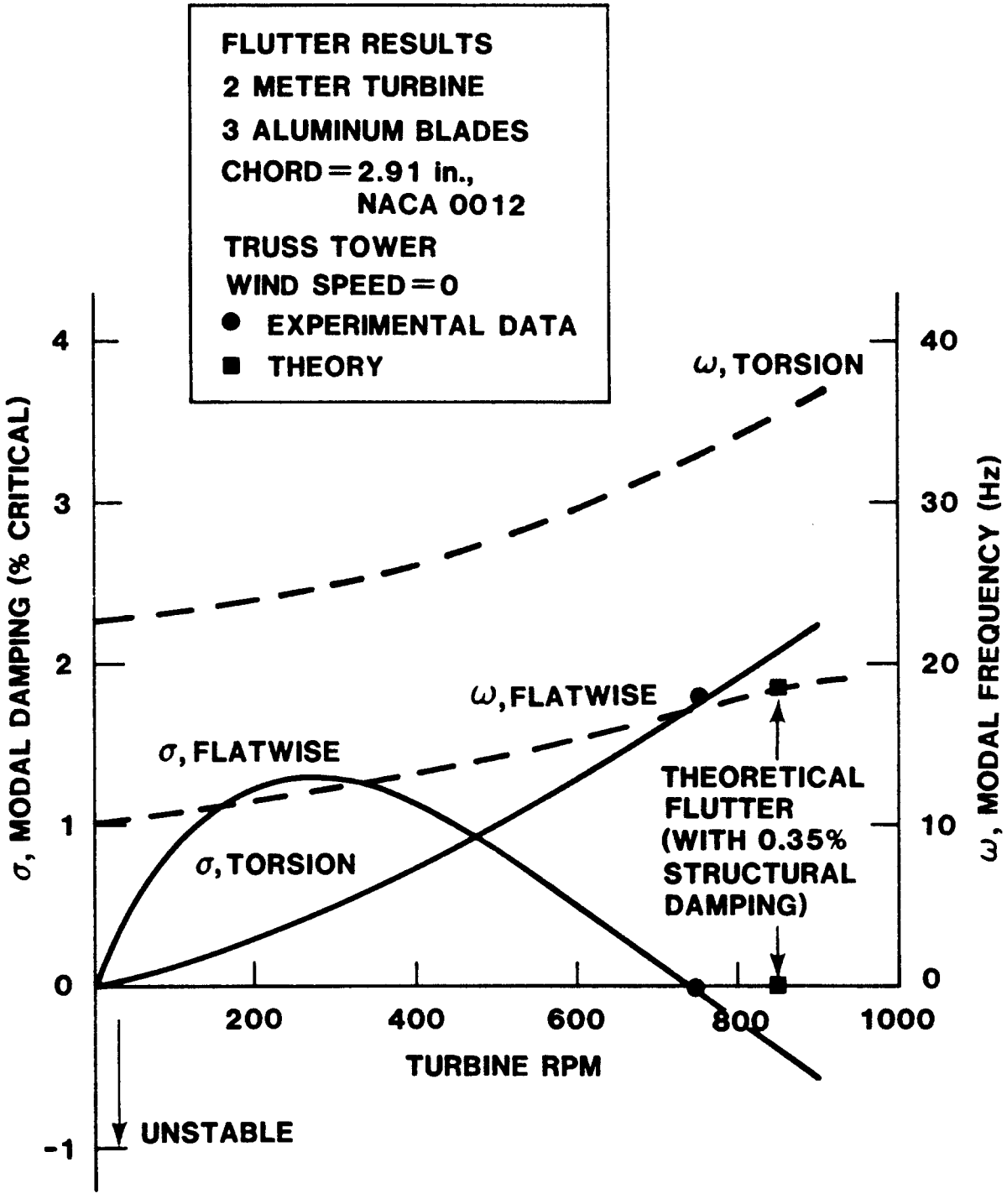

Figure 5. Comparison of Calculated and Measured Flutter Stability for the 2 Meter Turbine (NACA 0012, CHORD = 2.91 in)

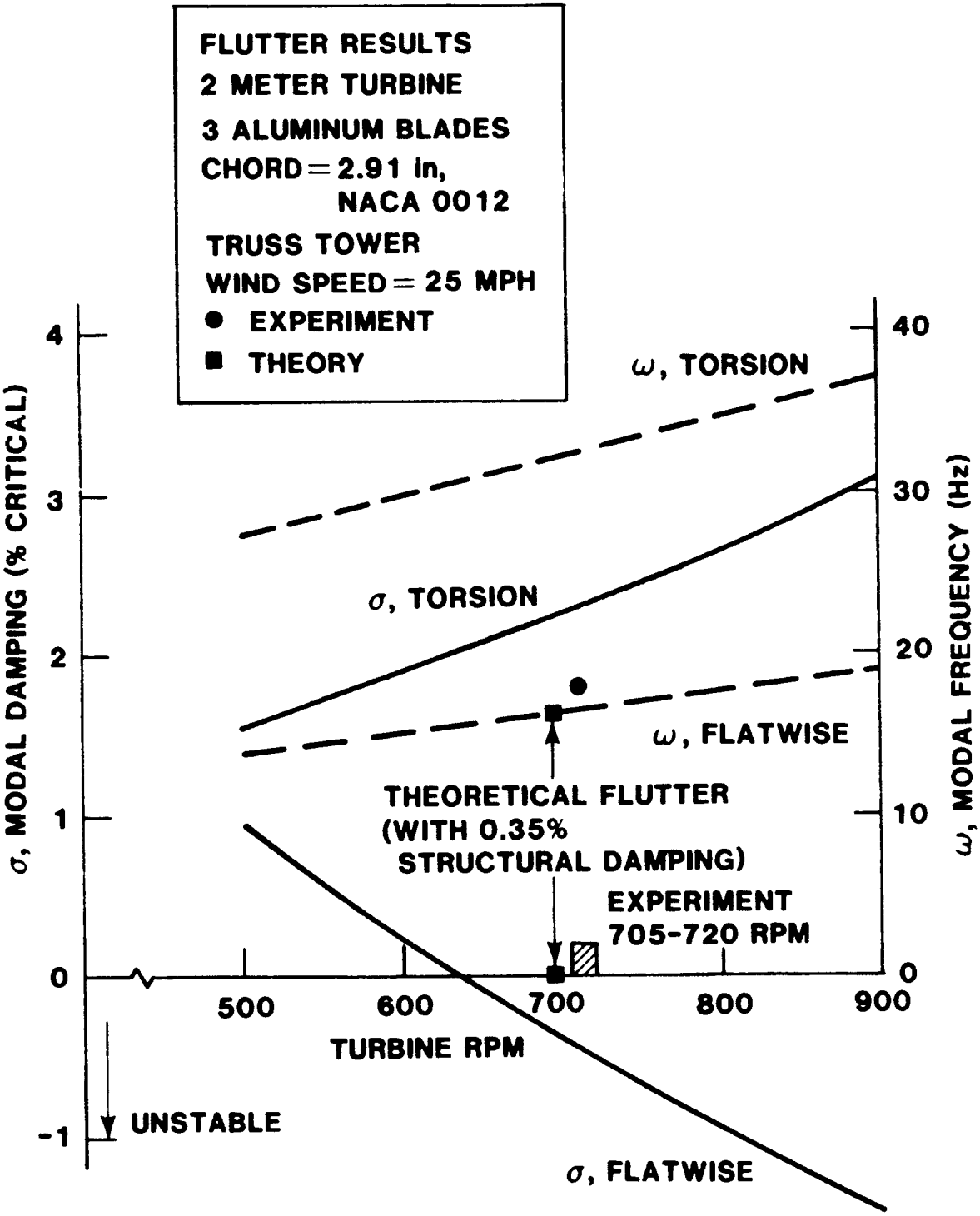

Figure 6. Effect of Wind Speed on Flutter Stability of the 2 Meter Turbine (NACA 0012, CHORD = 2.91 in)

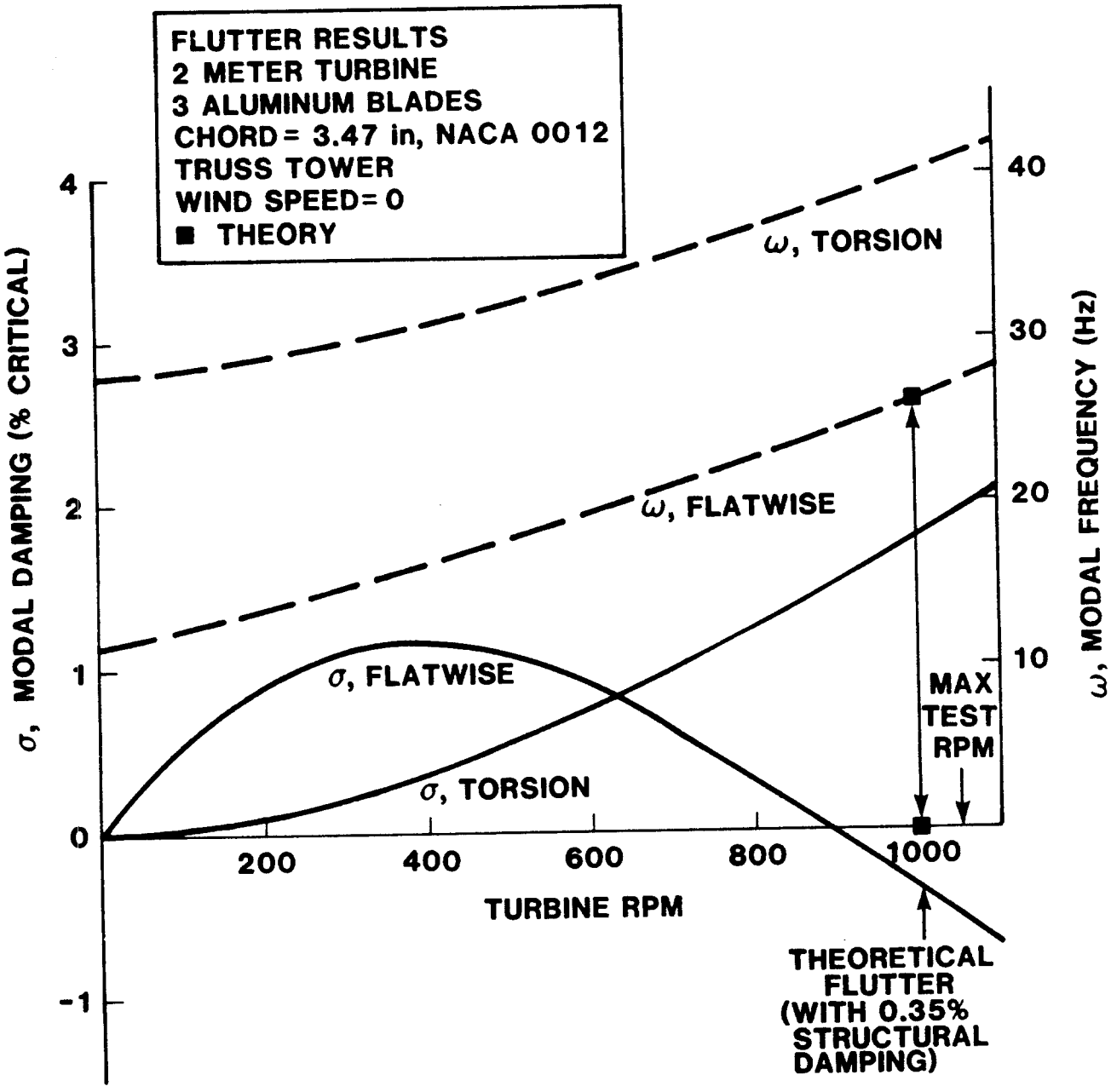

Figure 7. Comparison of Calculated and Measured Flutter Stability for the 2 Meter Turbine (NACA 0012, CHORD = 3.47 in)

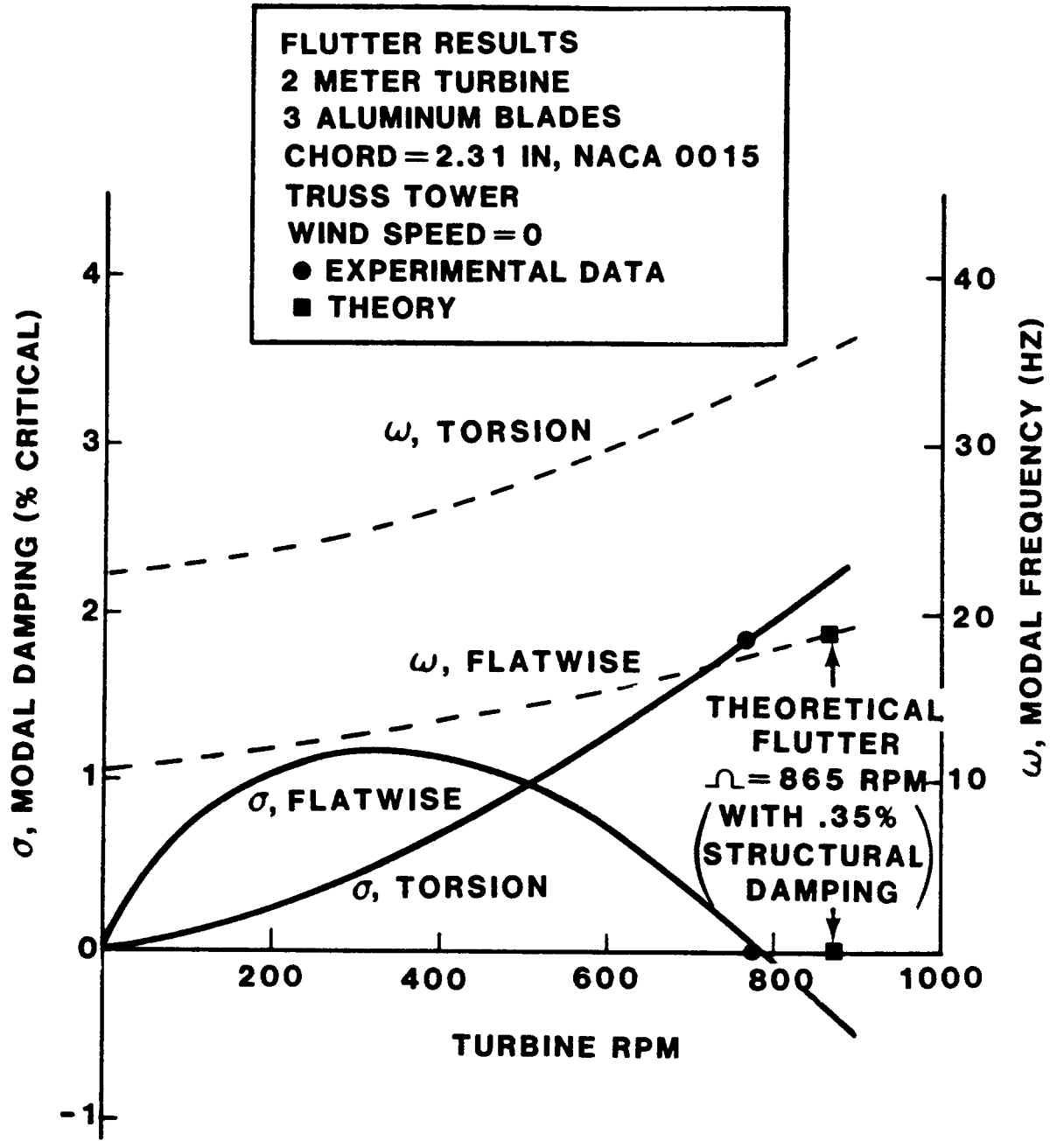

Figure 8. Comparison of Calculated and Measured Flutter Stability for the 2 Meter Turbine (NACA 0015, CHORD - 2.31 in)

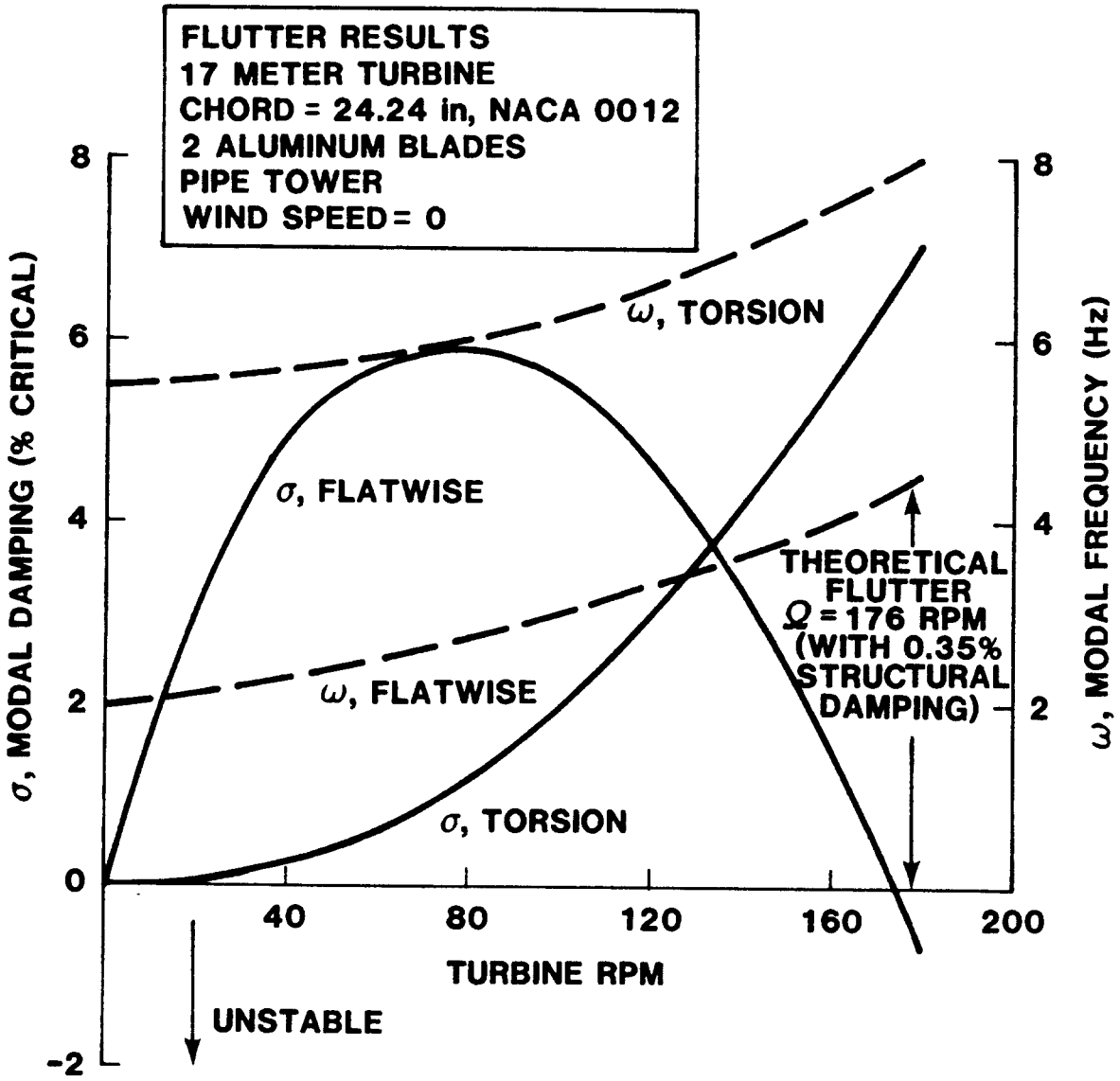

Figure 9. Flutter Stability Calculations for the 17 Meter Sandia Turbine

DISTRIBUTION:

Aero Engineering Department (2)
Wichita State University
Wichita, KS 67208
Attn: M. Snyder
W. Wentz

Alcoa Laboratories (4)
Alcoa Technical Center
Aluminum Company of America
Alcoa Center, PA 15069
Attn: D. K. Ai
A. G. Craig
J. T. Huang
J. R. Jombock

American Wind Energy Association
1609 Connecticut Avenue NW
Washington, DC 20009

E. E. Anderson
South Dakota School of Mines and Technology
Department of Mechanical Engineering
Rapid City, SD 57701

Scott Anderson
318 Millis Hall
University of Vermont
Burlington, VT 05405

Holt Ashley
Stanford University
Department of Aeronautics and
Astronautics Mechanical Engineering
Stanford, CA 94305

Kevin Austin
Consolidated Edison Company of
New York, Inc.
4 Irving Place
New York, NY 10003

B. H. Barksdale, Jr.
Hayes, Seay, Mattern, and Mattern
1315 Franklin Road SW
Roanoke, VA 24016

Dr. P. J. Baum
Institute of Geophysics
and Planetary Physics
University of California
Riverside, CA 92521

F. K. Bechtel
Washington State University
Department of Electrical Engineering
College of Engineering
Pullman, WA 99163

M. E. Beecher
Arizona State University
Solar Energy Collection
University Library
Tempe, AZ 85281

R. K. Berky
Alco Energy, Inc.
8002 Lee Blvd.
Leawood, KS 66208

Leon Bjervig
Civilingenior, MCIF
"Osterbyhus", 6990 Ulfborg
DK6990
DENMARK

K. Bergey
University of Oklahoma
Aero Engineering Department
Norman, OK 73069

Steve Blake
Wind Energy Systems
Route 1, Box 93-A
Oskaloosa, KS 66066

Robert Brulle
McDonnell-Douglas Aircraft Corporation
P.O. Box 516
Department 341, Building 32/2
St. Louis, MO 63166

R. Camerero
Faculty of Applied Science
University of Sherbrooke
Sherbrooke, Quebec
CANADA J1K 2R1

CERCEM
49 Rue du Commandant Rolland
93350 Le Bourget
FRANCE
Attn: J. Delassus

Professor V. A. L. Chasteau
School of Engineering
University of Auckland
Private Bag
Auckland, NEW ZEALAND

Howard T. Clark
McDonnell Aircraft Corporation
P.O. Box 516
Department 337, Building 32
St. Louis, MO 63166

Dr. R. N. Clark
USDA, Agricultural Research Service
Southwest Great Plains Research Center
Bushland, TX 79012

Joan D. Cohen
Consumer Outreach Coordinator
State of New York
Executive Department
State Consumer Protection Board
99 Washington Avenue
Albany, NY 12210

Dr. D. E. Cromack
Associate Professor
Mechanical and Aerospace Engineering
Department
University of Massachusetts
Amherst, MA 01003

DOE/ALO (2)
Albuquerque, NM 87115
Attn: G. P. Tennyson

DOE Headquarters/WETD (20)
1000 Independence Ave.
Room 5F067
Washington, DC 20585
Attn: W. C. Reddick

C. W. Dodd
School of Engineering
Southern Illinois University
Carbondale, IL 62901

D. D. Doerr
Kaiser Aluminum and Chemical Sales, Inc.
6177 Sunol Blvd.
P.O. Box 877
Pleasonton, CA 94566

Dominion Aluminum Fabricating Ltd. (2)
3570 Hawkestone Road
Mississauga, Ontario
CANADA L5C 2U8
Attn: L. Schienbein
C. Wood

D. P. Dougan
Hamilton Standard
1730 NASA Boulevard
Room 207
Houston, TX 77058

J. B. Dragt
Nederlands Energy Research Foundation (E.C.N.)
Physics Department
Westerduinweg 3 Patten (nh)
THE NETHERLANDS

C. E. Elderkin
Battelle-Pacific Northwest Laboratory
P.O. Box 999
Richland, WA 99352

Frank R. Eldridge, Jr.
The Mitre Corporation
1820 Dolley Madison Blvd.
McLean, VA 22102

Electric Power Research Institute
3412 Hillview Avenue
Palo Alto, CA 94304
Attn: E. Demeo

Energy Marketing Consultants, Inc.
Suite 1400
1100 Cleveland Ave.
Clearwater, FL 33515

Richard G. Ferreira, Chief
The Resources Agency
Department of Water Resources
Energy Division
1416 9th Street
P.O. Box 388
Sacremento, CA 95802

D. R. Finley
New England Geosystems
P.O. Box 128
East Derry, NH 03041

Flow Wind Corporation
21414 68th Avenue South
Kent, WA 98031
Attn: I. E. Vas

James D. Fock, Jr.
Department of Aerospace Engineering Sciences
University of Colorado
Boulder, CO 80309

G. A. Fontana (2)
Burns & Roe, Inc.
800 Kinderkamack Rd.
Oradell, NJ 07649

Dr. Lawrence C. Frederick
Public Service Company of New Hampshire
1000 Elm Street
Manchester, NH 03105

H. Gerardin
Mechanical Engineering Department
Faculty of Sciences and Engineering
Universite Laval-Quebec
CANADA G1K 7P4

E. Gilmore
Amarillo College
Amarillo, TX 79100

Paul Gipe
Wind Power Digest
P.O. Box 539
Harrisburg, PA 17108

Roger T. Griffiths
University College of Swansea
Department of Mechanical Engineering
Singleton Park
Swansea SA2 8PP
UNITED KINGDOM

Professor G. Gregorek
Ohio State University
Aeronautical and Astronautical Department
2070 Neil Avenue
Columbus, OH 43210

Richard Haddad
101 Arizona
P.O. Box 530
El Paso, TX 79944

A. A. Hagman
Kaiser Aluminum and Chemical Sales, Inc.
14200 Cottage Grove Avenue
Dolton, IL 60419

Martin L. Hally, Section Manager
Project Department
Electricity Supply
18 St. Stephen's Green
Dublin 2, IRELAND

Professor N. D. Ham
Massachusetts Institute of Technology
77 Massachusetts Avenue
Cambridge, MA 02139

C. F. Harris
Wind Engineering Corporation
Airport Industrial Area
Box 5936
Lubbock, TX 79415

W. L. Harris
Aero/Astro Department
Massachusetts Institute of Technology
Cambridge, MA 02139

Terry Healy (2)
Rockwell International
Rocky Flats Plant
P.O. Box 464
Golden, CO 80401

Helion, Inc.
Box 445
Brownsville, CA 95919

Don Hinrichsen
Associate Editor
AMBIO
KVA
Fack, S-10405
Stockholm
SWEDEN

Sven Hugosson
Box 21048
S. 100 31 Stockholm 21
SWEDEN

O. Igra
Department of Mechanical Engineering
Ben-Gurion University of the Negev
Beer-Sheva, ISRAEL

Indian Oil Corporation, Ltd.
Marketing Division
254-C, Dr. Annie Besant Road
Prabhadevi, Bombay-400025
INDIA

JBF Scientific Corporation
2 Jewel Drive
Wilmington, MA 01887
Attn: E. E. Johanson

Dr. Gary L. Johnson, P.E.
Electrical Engineering Department
Kansas State University
Manhattan, KS 66506

B. O. Kaddy, Jr.
Box 353
31 Union Street
Hillsboro, NH 03244

Kaman Aerospace Corporation
Old Windsor Road
Bloomfield, CT 06002
Attn: W. Batesol

R. L. Katzenberg
2820 Upton St. NW
Washington, DC 20008

Robert E. Kelland
The College of Trades and Technology
P.O. Box 1693
Prince Philip Drive
St. John°s, Newfoundland
CANADA A1C 5P7

S. King
Natural Power, Inc.
New Boston, NH 03070

Larry Kinnett
P.O. Box 6593
Santa Barbara, CA 93111

Richard H. Klein
KW Control Systms, Inc.
27727 Conestoga Dr.
Rolling Hills Estates, CA 90274

Samuel H. Kohler
272 Old Delp Road
Lancaster, PA 17602

O. Krauss
Michigan State University
Division of Engineering Research
East Lansing, MI 48824

Carol Lamb
2584 East Geddes Avenue
Littleton, CO 80122

Lawrence Livermore Laboratory
P.O. Box 808 L-340
Livermore, CA 94550
Attn: D. W. Dorn

M. Lechner
Public Service Company of New Mexico
P.O. Box 2267
Albuquerque, NM 87103

Kalman Nagy Lehoczky
Cort Adelers GT. 30
Oslo 2
NORWAY

George E. Lennox
Industry Director
Mill Products Division
Reynolds Metals Company
6601 West Broad Street
Richmond, VA 23261

J. Lerner
State Energy Commission
Research and Development Division
1111 Howe Avenue
Sacramento, CA 95825

Richard LeRoy
Energy Marketing Consultants
1100 Cleveland St.
Suite 1400
Clearwater, FL 33515

L. Liljidahl
Building 303
Agriculture Research Center
USDA
Beltsville, MD 20705

P. B. S. Lissaman
Aeroenvironment, Inc.
660 South Arroyo Parkway
Pasadena, CA 91105

Olle Ljungstrom
FFA, The Aeronautical Research Institute
Box 11021
S-16111 Bromma
SWEDEN

T. H. Logan
U.S. Turbine Corporation
Olde Courthouse Building
Canfield, OH 44406

J. B. Longendyck
Siltex
7 Capitol Drive
Moonachie, NJ 07074

Los Alamos Scientific Laboratories
P.O. Box 1663
Los Alamos, NM 87544
Attn: J. D. Balcomb Q-DO-T

Beatrice de Saint Louvent
Establissement d°Etudes et de Recherches
Meteorologigues
77, Rue de Serves
92106 Boulogne-Billancourt Cedex
FRANCE

Ernel L. Luther
Senior Associate
PRC Energy Analysis Co.
7600 Old Springhouse Rd.
McLean, VA 22101

L. H. J. Maile
48 York Mills Rd.
Willowdale, Ontario
CANADA M2P 1B4

E. L. Markowski
Motorola, Inc.
G.E.D.
Mail Drop 1429
8201 E. McDowell Rd.
P.O. Box 1417
Scottsdale, AZ 85252

Jacques R. Maroni
Ford Motor Company
Environmental Research and Energy
Planning Director
Environmental and Safety Engineering Staff
The American Road
Dearborn, MI 48121

Frank Matanzo
Dardalen Associates
15110 Frederick Road
Woodbine, MD 21797

H. S. Matsuda, Manager
Composite Materials Laboratory
Pioneering R&D Laboratories
Toray Industries, Inc.
Sonoyama, Otsu, Shiga
JAPAN 520

J. R. McConnell
Tumac Industries, Inc.
650 Ford St.
Colorado Springs, CO 80915

James Meiggs
Kaman Sciences Corporation
P.O. Box 7463
Colorado Springs, CO 80933

R. N. Meroney
Colorado State University
Department of Civil Engineering
Fort Collins, CO 80521

G. N. Monsson
Department of Economic Planning
and Development
Barrett Building
Cheyenne, WY 82002

Napier College of Commerce and Technology
Tutor Librarian, Technology Faculty
Colinton Road
Edinburgh, EH10 5DT
ENGLAND

NASA Lewis Research Center (4)
21000 Brookpark Road
Cleveland, OH 44135
Attn: K. Kaza
W. Robbins
J. Savino
R. L. Thomas

Anthony A. Nedd
The Power Company, Inc.
P.O. Box 221
Genesee Depot, WI 53217

V. Nelson
West Texas State University
Department of Physics
P.O. Box 248
Canyon, TX 79016

Leander Nichols
Natural Power, Inc.
New Boston, NH 03070

Ronald Nousain
P.O. Box 111
Rome 1132
Los Angeles, CA 90051

Roger O°Hara
Energy Times
909 NE 43rd
Suite 308
Seattle, WA 98105

Oklahoma State University (2)
Stillwater, OK 76074
Attn: W. L. Hughes
EE Department
D. K. McLaughlin
ME Department

Oregon State University (2)
Corvallis, OR 97331
Attn: R. W. Thresher
ME Department
R. E. Wilson
ME Department

Alcir de Faro Orlando
Pontificia Universidade Catolica-PUC/Rj
Mechanical Engineering Department
R. Marques de S. Vicente 225
Rio de Janeiro, BRAZIL

Pat F. O°Rourke
Precinct 4
County Commissioner
City-County Building
El Paso, TX 79901

H. H. Paalman
Dow Chemical USA
Research Center
2800 Mitchell Drive
Walnut Creek, CA 94598

Dr. Y. H. Pao, Chairman
Flow Industries, Inc.
21414 68th Ave. South
Kent, WA 98031

Ion Paraschivoiu
IREQ
1800 montee Ste-Julie
Varennes, Qeubec
CANADA JOL 2PO

Gary D. Park
Gates Learjet
Mid-Continent Airport
P.O. Box 7707
Wichita, KS 67277

R. A. Parmalee
Northwestern University
Department of Civil Engineering
Evanston, IL 60201

Helge Petersen
Riso National Laboratory
DK-4000 Roskilde
DENMARK

Wilson Prichett, III
National Rural Electric Cooperative
Association
1800 Massachusetts Avenue NW
Washington, DC 20036

K. R. Rasmussen
Utah Power and Light Co.
51 East Main St.
P.O. Box 277
American Fork, UT 84003

Dr. Barry Rawlings, Chief
Division of Mechanical Engineering
Commonwealth Scientific and Industrial
Research Organization
Graham Road, Highett
Victoria, 3190
AUSTRALIA

Thomas W. Reddoch
Associate Professor
Department of Electrical Engineering
The University of Tennessee
Knoxville, TN 37916

Ray G. Richards
Atlantic Wind Test Site
P.O. Box 189
Tignish P.E.I.
COB 2BO CANADA

A. Robb
Memorial University of Newfoundland
Faculty of Engineering and Applied Sciences
St. John°s Newfoundland
CANADA A1C 5S7

J. R. Rodriguez
Solarwind Energy Corporation
1163 Pomona Road
Unit A
Corona, CA 91720

Dr. -Ing. Hans Ruscheweyh
Institut fur Leichbau
Technische Hochschule Aachen
Wullnerstrasse 7
GERMANY

R. K. St. Aubin
Aerolite, Inc.
550 Russells Mills Rd.
South Dartmouth, MA 02748

Gwen Schreiner
Librarian
National Atomic Museum
Albuquerque, NM 87185

Douglas B. Seely, P.E.
U.S. Department of Energy
P.O. Box 3621
102 NE Holladay
Portland, OR 97208

Arnan Seginer
Professor of Aerodynamics
Technion-Israel Institute of
Technology
Department of Aeronautical
Engineering
Haifa, ISRAEL

Dr. Horst Selzer
Dipl.-Phys.
Wehrtechnik und Energieforschung
ERNO-Raumfahrttechnik GmbH
Hunefeldstr. 1-5
Postfach 10 59 09
2800 Bremen 1
GERMANY

H. Sevier
Rocket and Space Division
Bristol Aerospace Ltd.
P.O. Box 874
Winnipeg, Manitoba
CANADA R3C 2S4

P. N. Shankar
Aerodynamics Division
National Aeronautical Laboratory
Bangalore 560017
INDIA

David Sharpe
Kingston Polytechnic
Canbury Park Road
Kingston, Surrey
UNITED KINGDOM

D. G. Shepherd
Cornell University
Sibley School of Mechanical and
Aerospace Engineering
Ithaca, NY 14853

Dr. Fred Smith
Mechanical Engineering Department Head
Colorado State University
Ft. Collins, CO 80521

Kent Smith
Instituto Technologico Costa Rica
Apartado 159 Cartago
COSTA RICA

Leo H. Soderholm
Iowa State University
Agricultural Engineering, Room 213
Ames, IA 50010

Bent Sorenson
Roskilde University Centery
Energy JGroup, Bldg. 17.2
IMFUFA
P.O. Box 260
DK-400 Roskilde
DENMARK

Southwest Research Institute (2)
P.O. Drawer 28501
San Antonio, TX 78284
Attn: W. L. Donaldson, Senior Vice President
R. K. Swanson

Rick Stevenson
Route 2
Box 85
Springfield, MO 65802

Dale T. Stjernholm, P.E.
Mechanical Design Engineer
Morey/Stjernholm and Associates
1050 Magnolia Street
Colorado Springs, CO 80907

G. W. Stricker
130 Merchant St. #1104
Honolulu, HI 96813

C. J. Swet
Route 4
Box 358
Mt. Airy, MD 21771

John Taylor
National Research Council
ASEB
2101 Constitution Avenue
Washington, DC 20418

R. J. Templin (3)
Low Speed Aerodynamics Section
NRC-National Aeronautical Establishment
Ottawa 7, Ontario
CANADA K1A OR6

Texas Tech University (3)
P.O. Box 4389
Lubbock, TX 79409
Attn: J. Lawrence, ME Department
K. C. Mehta, CE Department
J. H. Strickland, ME Department

Fred Thompson
Atari, Inc.
155 Moffett Park Drive
Sunnyvale, CA 94086

F. M. Townsend
Aluminum Company of America
1501 Alcoa Building
Pittsburgh, PA 15219

J. M. Turner, Group Leader
Terrestrial Energy Technology Program Offic
Energy Conversion Branch
Aerospace Power Division
Aero Propulsion Laboratory
Department of the Air Force
Air Force Wright Aeronautical Laboratories
Wright-Patterson Air Force Base, OH 45433

United Engineers and Constructors, Inc.
Advanced Engineering Department
30 South 17th Street
Philadelphia, PA 19101
Attn: A. J. Karalis

University of New Mexico (2)
New Mexico Engineering Research Institute
Campus, P.O. Box 25
Albuquerque, N.M. 87131
Attn: G. G. Leigh

Jan Vacek
Eolienne experimentale
C.P. 279, Cap-aux-Meules
Iles de la Madeleine, Quebec
CANADA

Otto de Vries
National Aerospace Laboratory
Anthony Fokkerweg 2
Amsterdam 1017
THE NETHERLANDS

R. Walters
West Virginia University
Department of Aero Engineering
1062 Kountz Avenue
Morgantown, WV 26505

E. J. Warchol
Bonneville Power Administration
P.O. Box 3621
Portland, OR 97225

D. F. Warne, Manager
Energy and Power Systems
ERA Ltd.
Cleeve Rd.
Leatherhead
Surrey KT22 7SA
ENGLAND

G. R. Watson, Project Manager
The Energy Center
Pennine House
4 Osborne Terrace
Newcastle upon Tyne NE2 1NE
UNITED KINGDOM

R. J. Watson
Watson Bowman Associates, Inc.
1280 Niagara St.
Buffalo, NY 14213

Tom Watson
Canadian Standards Association
178 Rexdale Blvd.
Rexdale, Ontario
CANADA M9W 1R3

R. G. Watts
Tulane University
Department of Mechanical Engineering
New Orleans, LA 70018

W. G. Wells, P.E.
Associate Professor
Mechanical Engineering Department
Mississippi State University
Mississippi State, MS 39762

T. Wentink, Jr.
University of Alaska
Geophysical Institute
Fairbanks, AK 99701

West Texas State University
Government Depository Library
Number 613
Canyon, TX 79015

Wind Energy Report
Box 14
102 S. Village Ave.
Rockville Centre, NY 11571
Attn: Farrell Smith Seiler

Wind Program Manager
Wisconsin Division of State Energy
8th Floor
101 South Webster Street
Madison, WI 53702

Richard E. Wong
Assistant Director
Central Solar Energy Research Corp.
1200 Sixth Street
328 Executive Plaza
Detroit, MI 48226

David Popelka (15)
Bell Helicopter
P. O. Box 482
Ft. Worth, TX 76101

1000 G. A. Fowler
1200 L. D. Smith
2525 R. P. Clark
3161 J. E. Mitchell (15)
3161 P. S. Wilson
4533 J. W. Reed
4700 E. H. Beckner
4720 D. G. Schueler
4725 R. H. Braasch
4725 R. E. Akins
4725 J. D. Cyrus
4725 R. D. Grover
4725 E. G. Kadlec
4725 P. C. Klimas
4725 M. T. Mattison
4725 R. O. Nellums
4725 W. N. Sullivan
4725 R. A. Watson
4725 M. H. Worstell
5500 O. E. Jones
5510 D. B. Hayes
5520 T. B. Lane
5523 R. C. Reuter, Jr.
5523 D. B. Clauss
5523 D. W. Lobitz
5523 P. S. Veers
5530 W. Herrmann
5600 D. B. Shuster
5620 M. M. Newsom
5630 R. C. Maydew
5533 R. E. Sheldahl
5636 J. K. Cole
5636 D. E. Berg
5636 W. H. Curry
8214 M. A. Pound
3141 L. J. Erickson (5)
3151 W. L. Garner (3)
3154-3 C. H. Dalin (25)
For DOE/TIC (Unlimited Release)

Reprinted July, 1983
1523 W. N. Sullivan (25)

Reprinted November 1984 (50)